

Linear Decrease in the Magnetocrystalline Anisotropy*

C. ABRAHAM AND A. AHARONI

Department of Electronics, The Weizmann Institute of Science, Rehovoth, Israel

(Received July 18, 1960)

In a previous paper, an attempt was made to reduce the theoretical coercive force by assuming that the magnetocrystalline anisotropy constant vanished in a certain region. A modification of this assumption was made in the present work, namely, the magnetocrystalline anisotropy was taken as zero in a part of the "imperfection" region and assumed to increase linearly to its constant value in the remaining part. The coercive force is calculated as a function of two parameters: the dimensions of the zero and linear parts of the imperfection region. A further reduction in the coercive force was obtained with respect to the previous case, but there is still a large discrepancy between the calculated and experimental values, for reasonable defect size.

I. INTRODUCTION

THE present work is based on Rathenau *et al.*'s suggestions,¹ that domain walls might nucleate at regions where, for some defect of structure, the local magnetocrystalline anisotropy constant is low. In a previous paper,² it was shown that it is not sufficient for $\bar{K}(x)$, the magnetocrystalline anisotropy, to be a step function, with a jump from zero to K . A gradual change from zero to K seems to be needed. Therefore, a linear change is assumed here.

More specifically, a ferromagnetic material, infinite in all directions, which has an uniaxial magnetocrystalline anisotropy $\bar{K}(x)$, is considered. The external field is in the direction of the z axis, which is taken also as the direction of easy magnetization.

This implies that the direction cosines of the magnetization vector are:

$$\alpha_x = 0, \quad \alpha_y = \sin\omega, \quad \alpha_z = \cos\omega,$$

where ω is a function of x only. Minimizing the energy,² one obtains the following differential equation for ω .

$$2Ad^2\omega/dx^2 - \bar{K}(x) \sin 2\omega - HI_s \sin\omega = 0. \quad (1a)$$

Here A is the exchange constant and I_s the saturation magnetization. $\bar{K}(x)$ is assumed to have the symmetry property

$$\bar{K}(x) = \bar{K}(-x),$$

and to be of the form

$$\bar{K}(x) = \begin{cases} 0 & \text{if } 0 \leq x \leq d \\ K(x-d)/md & \text{if } d \leq x \leq d+md. \\ K & \text{if } d+md \leq x \end{cases} \quad (1b)$$

Using (1b) one can write the differential equation (1a) in the form:

$$d^2\omega/dt^2 + T^2h \sin\omega = 0, \quad 0 \leq t \leq 1, \quad (2a)$$

* This work will be included in a thesis by C. Abraham to be submitted to the Hebrew University, Jerusalem, in partial fulfillment of the requirements for a degree of Doctor of Philosophy.
¹ G. W. Rathenau, J. Smit, and A. L. Stuyts, *Z. Physik* **133**, 250 (1952).

² A. Aharoni, *Phys. Rev.* **119**, 127 (1960).

$$d^2\omega/dt^2 + T^2h \sin\omega + T^2[(1-t)/2m] \sin 2\omega = 0, \quad 1 \leq t \leq 1+m, \quad (2b)$$

$$d^2\omega/dt^2 + T^2h \sin\omega - \frac{1}{2}T^2 \sin 2\omega = 0, \quad 1+m \leq t, \quad (2c)$$

where

$$t = x/d, \quad h = -HI_s/2K, \quad T = dK^{\frac{1}{2}}A^{-\frac{1}{2}}. \quad (3)$$

ω and its derivative are continuous everywhere (including the points $t=1$, $t=1+m$), while the boundary conditions are:

$$\omega'(0) = \omega'(\infty) = 0. \quad (4)$$

The reduced field h defined in (3) is given in terms of $2K/I_s$, which is the coercive force for perfect material. Therefore, solutions of (2) are sought only for $h < 1$.

II. THE NUCLEATION FIELD

If one starts with a material magnetized in the $+z$ direction, reducing the field subsequently, a value h_n of h is found, at which the saturation solution $\omega=0$, becomes unstable. Since any change is small when it just starts, (2) may be written at nucleation in the form:

$$\omega'' + T^2h\omega = 0, \quad 0 \leq t \leq 1, \quad (5a)$$

$$m\omega'' + T^2(1+mh-t)\omega = 0, \quad 1 \leq t \leq 1+m, \quad (5b)$$

$$\omega'' + T^2(h-1)\omega = 0, \quad 1+m \leq t. \quad (5c)$$

The solutions of (5) for which the boundary conditions (4) hold, are:

$$\omega = C \cos Th^{\frac{1}{2}}t, \quad 0 \leq t \leq 1 \quad (6a)$$

$$\omega = \left(\frac{1+mh-t}{m}\right)^{\frac{1}{2}} \left\{ A_1 J_{\frac{1}{2}} \left(\frac{2mT}{3} \left[\frac{1+mh-t}{m} \right]^{\frac{3}{2}} \right) + B_1 J_{-\frac{1}{2}} \left(\frac{2mT}{3} \left[\frac{1+mh-t}{m} \right]^{\frac{3}{2}} \right) \right\}, \quad 1 \leq t \leq 1+mh, \quad (6b1)$$

$$\omega = \left(\frac{1+mh-t}{m}\right)^{\frac{1}{2}} \left\{ A_2 J_{\frac{1}{2}} \left(\frac{2mT}{3} \left[\frac{1+mh-t}{m} \right]^{\frac{3}{2}} \right) + B_2 J_{-\frac{1}{2}} \left(\frac{2mT}{3} \left[\frac{1+mh-t}{m} \right]^{\frac{3}{2}} \right) \right\}, \quad 1+mh \leq t \leq 1+m, \quad (6b2)$$

$$\omega = D \exp[-T(1-h)^{3/2}t], \quad 1+m \leq t. \quad (6c)$$

Here, $A_i, B_i (i=1, 2), C$ and D are constants, and J is the Bessel function of the first kind. From the continuity of ω and ω' at $t=1+mh$, we get for (6b):

$$A_1 = -A_2 = A, \quad B_1 = B_2 = B,$$

so that

$$\omega = \left(\frac{1+mh-t}{m}\right)^{3/2} \left\{ AJ_{3/2} \left(\frac{2mT}{3} \left[\frac{1+mh-t}{m} \right]^{3/2} \right) + BJ_{-3/2} \left(\frac{2mT}{3} \left[\frac{1+mh-t}{m} \right]^{3/2} \right) \right\}, \quad 1 \leq t \leq 1+mh, \quad (7b1)$$

$$\omega = \left(\frac{t-1-mh}{m}\right)^{3/2} \left\{ -AI_{3/2} \left(\frac{2mT}{3} \left[\frac{t-1-mh}{m} \right]^{3/2} \right) + BI_{-3/2} \left(\frac{2mT}{3} \left[\frac{t-1-mh}{m} \right]^{3/2} \right) \right\}, \quad 1+mh \leq t \leq 1+m. \quad (7b2)$$

TABLE I. The reduced nucleation field h_n as function of the two defect size parameters T and m defined in the text.

| $\frac{m}{T}$ | 0 | 1 | 2 | 4 |
|---------------|-------|-------|-------|-------|
| 1 | 0.546 | 0.388 | 0.305 | 0.224 |
| 2 | 0.265 | 0.171 | 0.136 | 0.104 |
| 3 | 0.152 | 0.098 | 0.080 | 0.063 |

Here I is the modified Bessel function of the first kind. Using again smoothness of ω at the points $t=1, t=1+m$, the following equations are obtained:

$$C \cos \gamma = h^{3/2} [AJ_{3/2}(\alpha) + BJ_{3/2}(\alpha)],$$

$$C \sin \gamma = h^{3/2} [AJ_{-3/2}(\alpha) - BJ_{-3/2}(\alpha)], \quad t=1 \quad (8a)$$

$$D \exp[-T(1-h)^{3/2}] = (1-h)^{3/2} \times [-AI_{3/2}(\beta) + BI_{-3/2}(\beta)], \quad t=1+m \quad (8b)$$

$$D \exp[-T(1-h)^{3/2}] = (1-h)^{3/2} \times [AI_{-3/2}(\beta) - BI_{-3/2}(\beta)],$$

where

$$\alpha = 2mTh^{3/2}/3, \quad \beta = 2mT(1-h)^{3/2}/3, \quad \gamma = Th^{3/2}. \quad (9)$$

Equating to zero the determinant of the coefficients of $A, B, C,$ and D in (8) yields the following transcendental equation for $\alpha, \beta,$ and γ :

$$\tan \gamma = \frac{J_{-3/2}(\alpha)[I_{-3/2}(\beta) + I_{3/2}(\beta)] - J_{3/2}(\alpha)[I_{3/2}(\beta) + I_{-3/2}(\beta)]}{J_{3/2}(\alpha)[I_{-3/2}(\beta) + I_{3/2}(\beta)] + J_{-3/2}(\alpha)[I_{3/2}(\beta) + I_{-3/2}(\beta)]}. \quad (10)$$

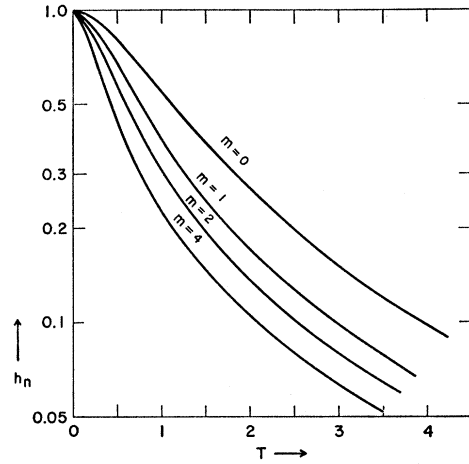


FIG. 1. The nucleation field in terms of the coercive force of perfect material, $2K/I$, as function of the defect size parameters T and m defined in the text.

Inverting (9),

$$h = [1 + (\beta/\alpha)^2]^{-1}, \quad (11a)$$

$$m = (3\alpha/4\gamma)[1 + (\beta/\alpha)^2], \quad (11b)$$

$$T = [1 + (\beta/\alpha)^2]^{3/2}. \quad (11c)$$

The form of (10) compelled us to proceed as follows: Arbitrary values of α and β were introduced in (10) subject only to the restriction that the values of γ found in this way should belong to the same branch of $\tan \gamma$.

Some graphs of T versus m were plotted, where only those triplets (α, β, γ) were considered, for which $\beta/\alpha = \text{const}$ [that is $h = \text{constant}$, as seen from, (11a)]. From these graphs, h_n was plotted as a function of T ,

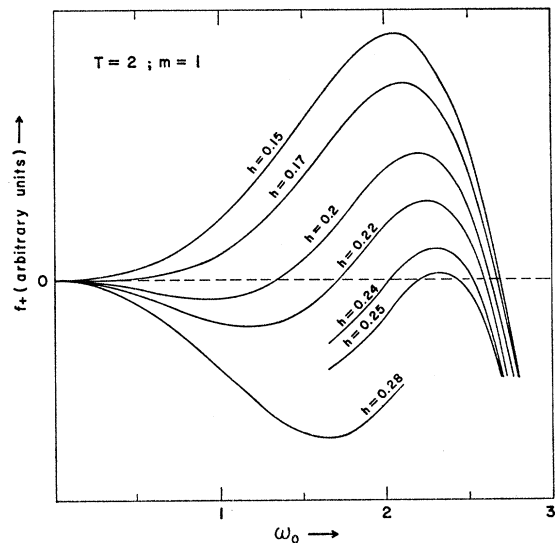


FIG. 2. The auxiliary function f^+ (in arbitrary units) in terms of the initial parameters ω_0 , for different values of the reduced field h and for $T=2, m=1$.

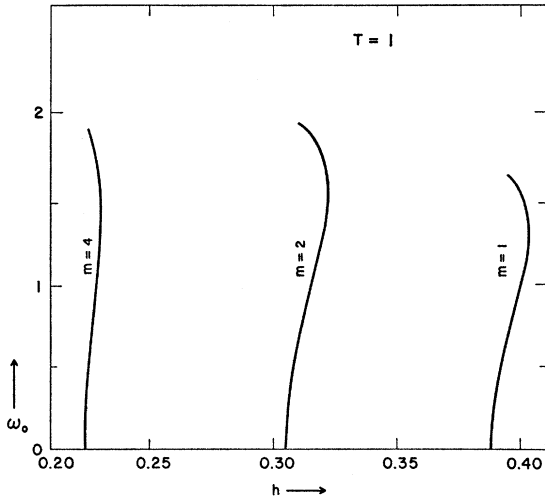


FIG. 3. The values of ω at $t=0$, as found from the zeroes of f^+ , plotted as function of the reduced field h , for $T=1$ and different values of m shown in the figure. The value of h at $\omega_0=0$ is the reduced nucleation field h_n . The reduced coercive force h_c is the value of h at the turning point of $\omega_0=\omega_0(h)$.

each plot corresponding to a certain value of m . The results are plotted in Fig. 1 and summarized in Table I.

III. SOLUTIONS OF THE DIFFERENTIAL EQUATIONS

Departing from the nucleation field, the stationary states of the physical system are represented by the solutions of the nonlinear equations (2), with ω and ω' continuous everywhere and fulfilling (4).

The solution of (2a) and (4) is:

$$\omega = -2 \arctan \left(\frac{k}{k'} \right) \text{cn}(Th^{1/2}t, k) \quad (12a)$$

[which is equivalent to (14a) of the previous paper²].

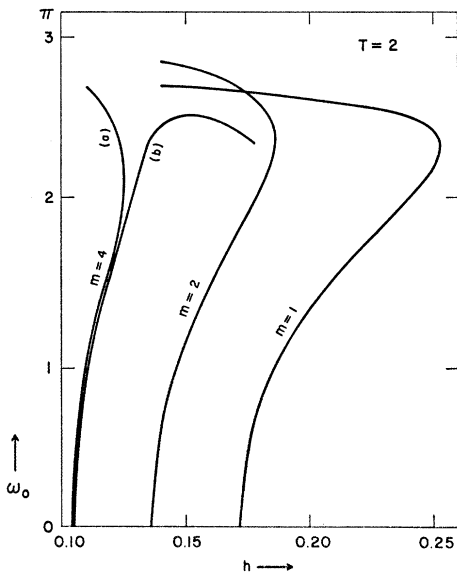


FIG. 4. Same as Fig. 3 for $T=2$.

Here cn is the cosine amplitude function,³ and

$$k = \sin(\omega_0/2), \quad k' = (1-k^2)^{1/2},$$

where ω_0 is the value of ω at $t=0$ and is a parameter of the integration. For $t \geq 1+m$ (2c) reduces to the equation

$$(\omega')^2 + \frac{1}{2}T^2 \cos 2\omega - 2T^2 h \cos \omega = D, \quad (12c)$$

where D is a constant.

Since $\omega_e=0$ and $\omega_e=\pi$ are the envelope singular solutions for all values of t , the constant D may be determined from the conditions

$$\omega_e=0, \pi, \quad \omega_e'=0.$$

It follows that the following equations have to be considered:

$$(\omega')^2 = T^2 [\sin^2 \omega + 2h(\cos \omega - 1)], \quad \text{for } \omega_e=0, \quad (13a)$$

$$(\omega')^2 = T^2 [\sin^2 \omega + 2h(\cos \omega + 1)], \quad \text{for } \omega_e=\pi. \quad (13b)$$

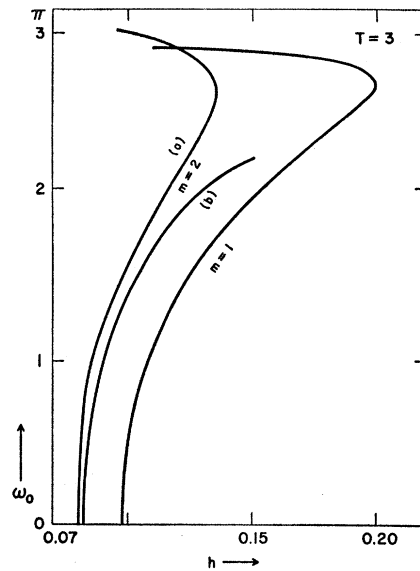


FIG. 5. Same as Fig. 3 for $T=3$.

The solutions of (13) are, respectively:

$$\omega = 2 \arctan \frac{2(h^{-1}-1)^{1/2} \exp[-T(1-h)^{1/2}(t+D_1)]}{1 + \exp[-2T(1-h)^{1/2}(t+D_1)]}, \quad \omega_e=0, \quad (14a)$$

$$\omega = 2 \arctan \left(\frac{h}{1+h} \right)^{1/2} \sinh [T(1+h)(t+D_2)], \quad \omega_e=\pi. \quad (14b)$$

Here D_1 and D_2 are constants.

Since the solutions of (2b) cannot be expressed in terms of known functions, a numerical solution was undertaken, using the fourth-order Runge-Kutta method. The numerical solution was started at $t=0$,

³ P. F. Byrd and M. D. Friedman, *Handbook of Elliptic Integrals for Engineers and Physicists* (Springer-Verlag, Berlin, 1954).

since this was considered easier than the programming of the solution (12a) for the first region. The Runge-Kutta method requires initial conditions, therefore $\omega_0 = \omega(0)$ was used as a parameter while $\omega'(0)$ is given in (4). The computations were done on the WEIZAC, the electronic computer of this Institute. In the actual computations, the following definitions were found useful:

$$f_+ = T^2[\sin^2\omega + 2h(\cos\omega - 1)] - (\omega')^2, \text{ for } \omega_e = 0, \quad (15a)$$

$$f_- = T^2[\sin^2\omega + 2h(\cos\omega + 1)] - (\omega')^2, \text{ for } \omega_e = \pi. \quad (15b)$$

For given values of T , h , and m , the values of ω_0 for which f_+ or f_- vanish at $t = 1 + m$ give solutions of (2), according to (13). The values of $f_+(1+m)$ and $f_-(1+m)$ were plotted as functions of ω_0 . An example of this plot is given in Fig. 2. From this and similar plots, the zeroes of f_+ were read. These are plotted as function as ω_0 in Figs. 3-6. No zeroes were found for f_- .

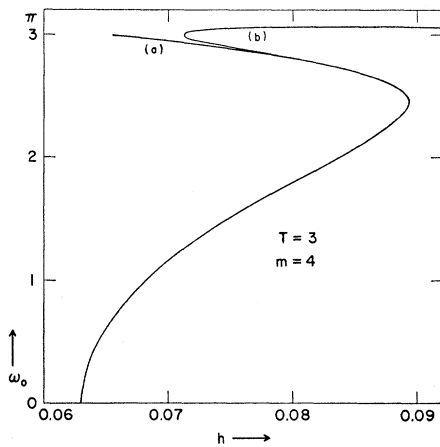


FIG. 6. Same as Fig. 3 for $T=3$, $m=4$.

Starting from nucleation, the solution can follow the values of ω_0 in Fig. 3 (the case $T=1$) for increasing values of h , until it reaches the turning point in which it must jump to the solution $\omega \equiv \pi$. This value of h is therefore the coercive force, since the magnetization in the finite defective regions does not influence the average magnetization and remains $+1$ up to this point, the hysteresis curve being rectangular. In Fig. 4 the case $T=2$ is plotted. Here, for $m=4$ one obtains 2 branches (a) and (b) (which appear together in constant h plots similar to Fig. 2). However, these start at different nucleation field and since the one for (a) is lower, the physical system starts on it and can never reach the solution (b), as is seen from the figure. The case $T=3$, $m=2$ in Fig. 5 is similar, while for $m=1$ one obtains a single branch. More complicated is the case $T=3$, $m=4$ (Fig. 6). Here the branch (b) starts at a higher nucleation field than (a) but appears above (a) at the turning point of the latter, so that the jump

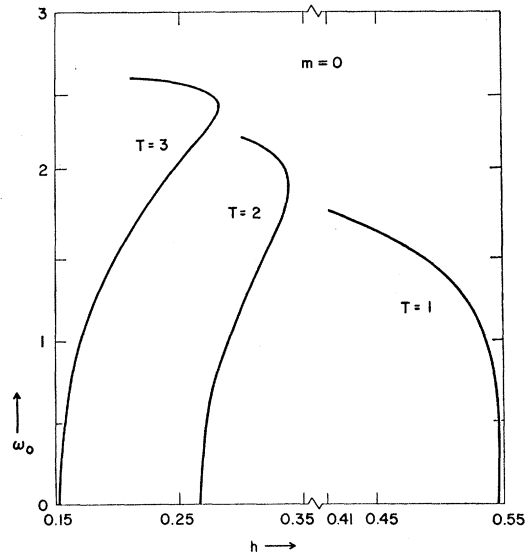


FIG. 7. Same as Fig. 3 for $m=0$ and different values of T .

TABLE II. The reduced coercive force h_c as function of the two defect size parameters T and m .

| $T \backslash m$ | 0 | 1 | 2 | 4 |
|------------------|-------|-------|-------|-------|
| 1 | 0.546 | 0.403 | 0.321 | 0.230 |
| 2 | 0.339 | 0.253 | 0.186 | 0.125 |
| 3 | 0.283 | 0.199 | 0.136 | 0.089 |

could in principle be to (b) rather than to the solution $\omega \equiv \pi$. However, the (b) solutions in this case were found out to be related to negative values of ω in $t = 1 + m$ which is impossible according to (14a). The curve (b) is therefore a parasitic solution introduced because of the form of (15a) and has no physical meaning. The coercive force in Fig. 6 is therefore the turning point of (a) as in previous cases. In Fig. 7 the case $m=0$ is plotted, i.e., the case discussed in the previous paper.²

The coercive force thus calculated is given in Table II.

IV. CONCLUSIONS

The addition of linear region to the step function in \bar{K} does not change considerably the nucleation field. However, the coercive force is considerably reduced. One order of magnitude reduction of the theoretical coercive force is obtained for rather small defect size. Yet this model does not seem to be sufficient to explain the experimental data. Only if superposition of imperfections of similar type will prove to reduce the coercive force much further can this model be expected to approach the physical case.

ACKNOWLEDGMENT

The authors are much indebted to Professor E. H. Frei under whom this work has been carried out.